Supporting Information

Enhancing Propylene/Propane Separation Performances of ZIF-8 Membranes by Post-Synthetic Surface Polymerization

Sunghwan Park[a], Kie Yong Cho[b] and Hae-Kwon Jeong*[,a,c]

[a] *Artie McFerrin Department of Chemical Engineering and* [c] *Department of Materials Science and Engineering, Texas A&M University, 3122 TAMU, College Station, TX 77843-3122, United States*

[b] *Department of Industrial Chemistry, Pukyong National University, 45 Yongso-ro, Nam-gu, Busan 48513, Republic of Korea*

* *Corresponding author:*

H.-K. Jeong (e-mail address: hjeong7@tamu.edu, Phone: +1-979-862-4850, Fax: +1-979-845-6446)

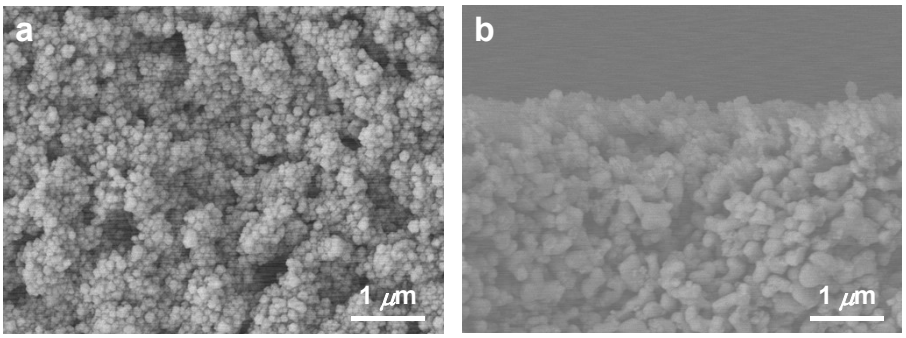

Figure S1. SEM images of a ZIF-8 seed layer: **a** top view and **b** cross-sectional view.

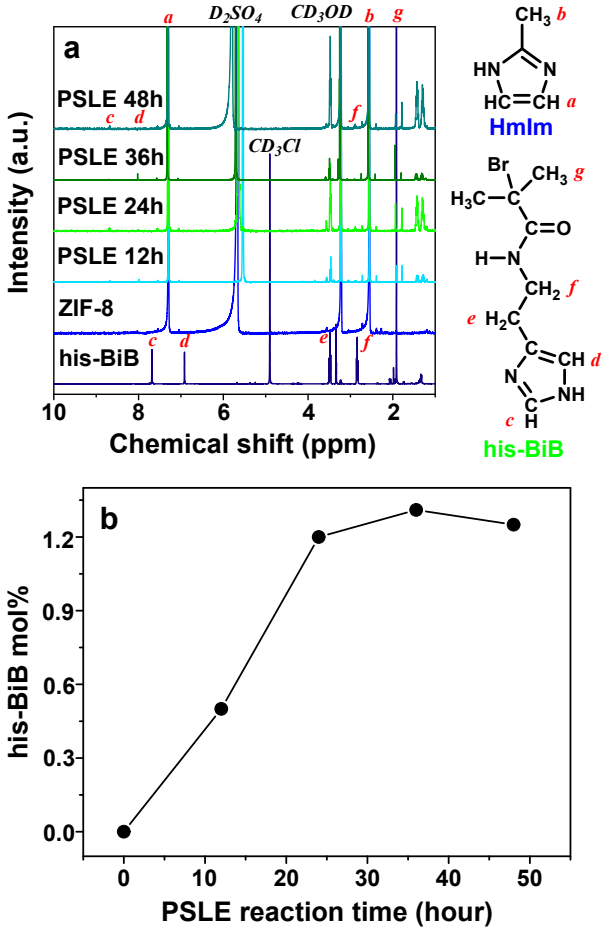

Figure S2. a ^{1}H NMR spectra of his-BiB, ZIF-8, and ZIF-8-BiB membranes and **b** his-BiB contents of ZIF-8-BiB membranes as a function of different PSLE reaction times. The unidentified signals in (a) are attributed to TEA·HBr salt as a byproduct.

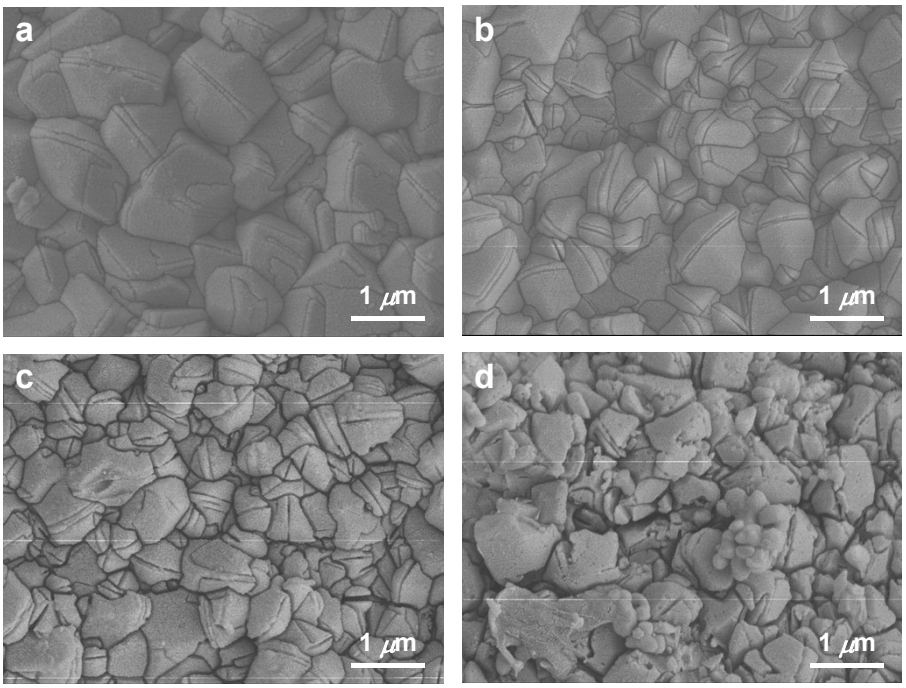

Figure S3. SEM images of ZIF-8-BiB membranes treated for different PSLE times: **a** 12 h , **b** 24 h, **c** 36 h, and **d** 48 h.

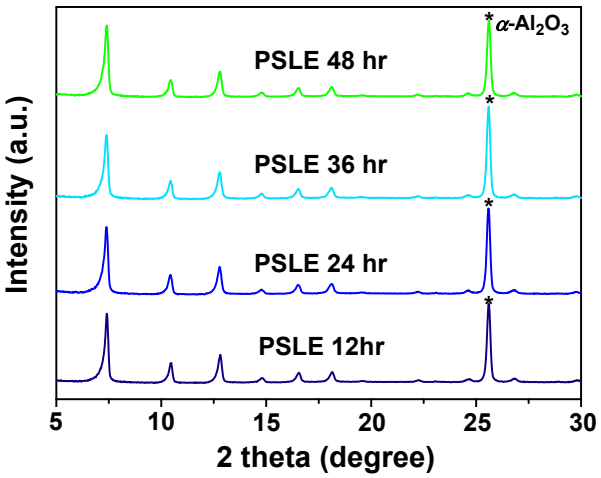

Figure S4. Diffraction patterns of ZIF-8-BIB membranes for different PSLE times.

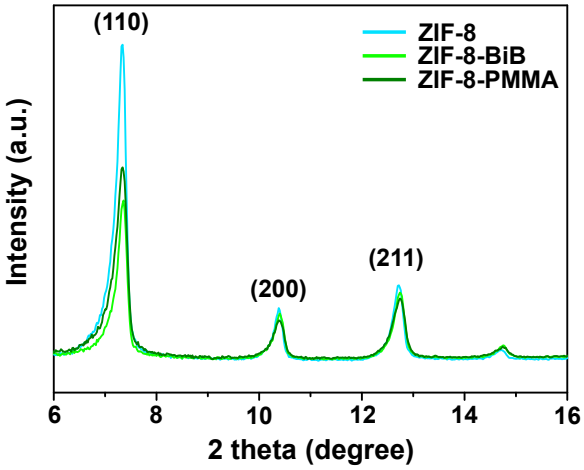

Figure S5. PXRD patterns of a ZIF-8 membrane, a ZIF-8-BiB membrane, and a ZIF-8-PMMA membrane.

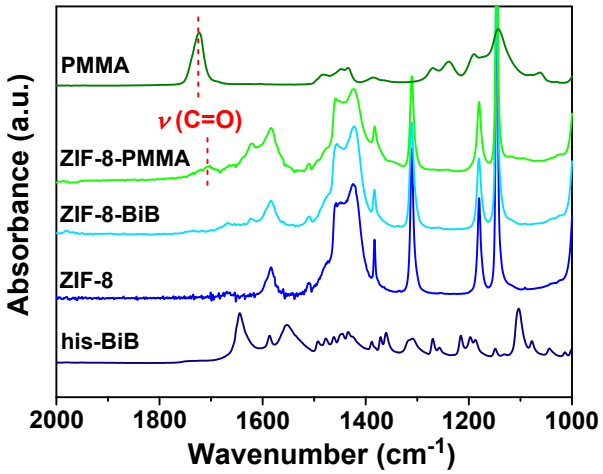

Figure S6. FT-IR spectra of his-BiB, bulk PMMA, ZIF-8 membrane, ZIF-8-BiB membrane, and ZIF-8-PMMA membrane.

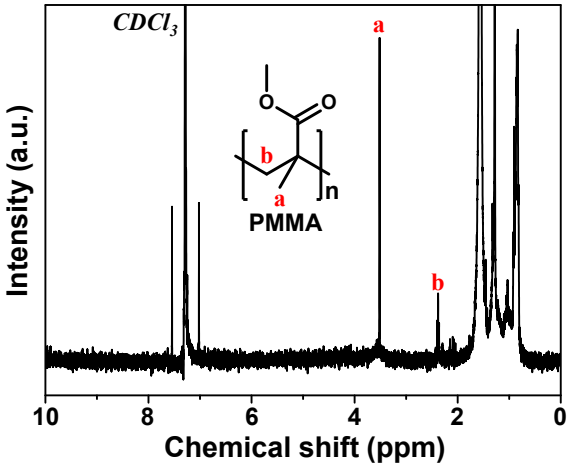

Figure S7. ^{1}H NMR spectrum of PMMA obtained from a digested ZIF-8-PMMA membrane.

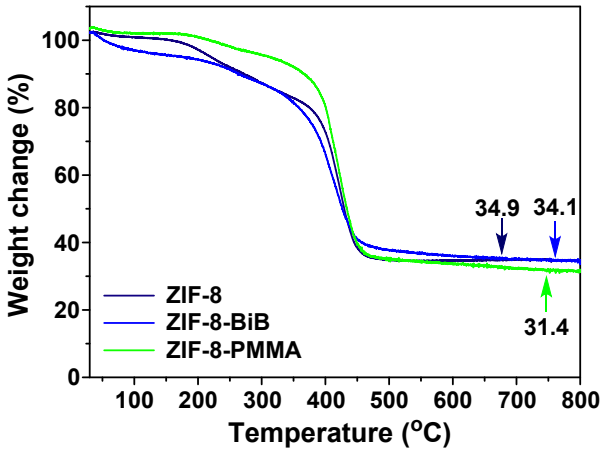

Figure S8. Thermograms of ZIF-8, ZIF-8-BiB, and ZIF-8-PMMA membranes. Note that the weight of the α-Al_2O_3 substrate was subtracted.

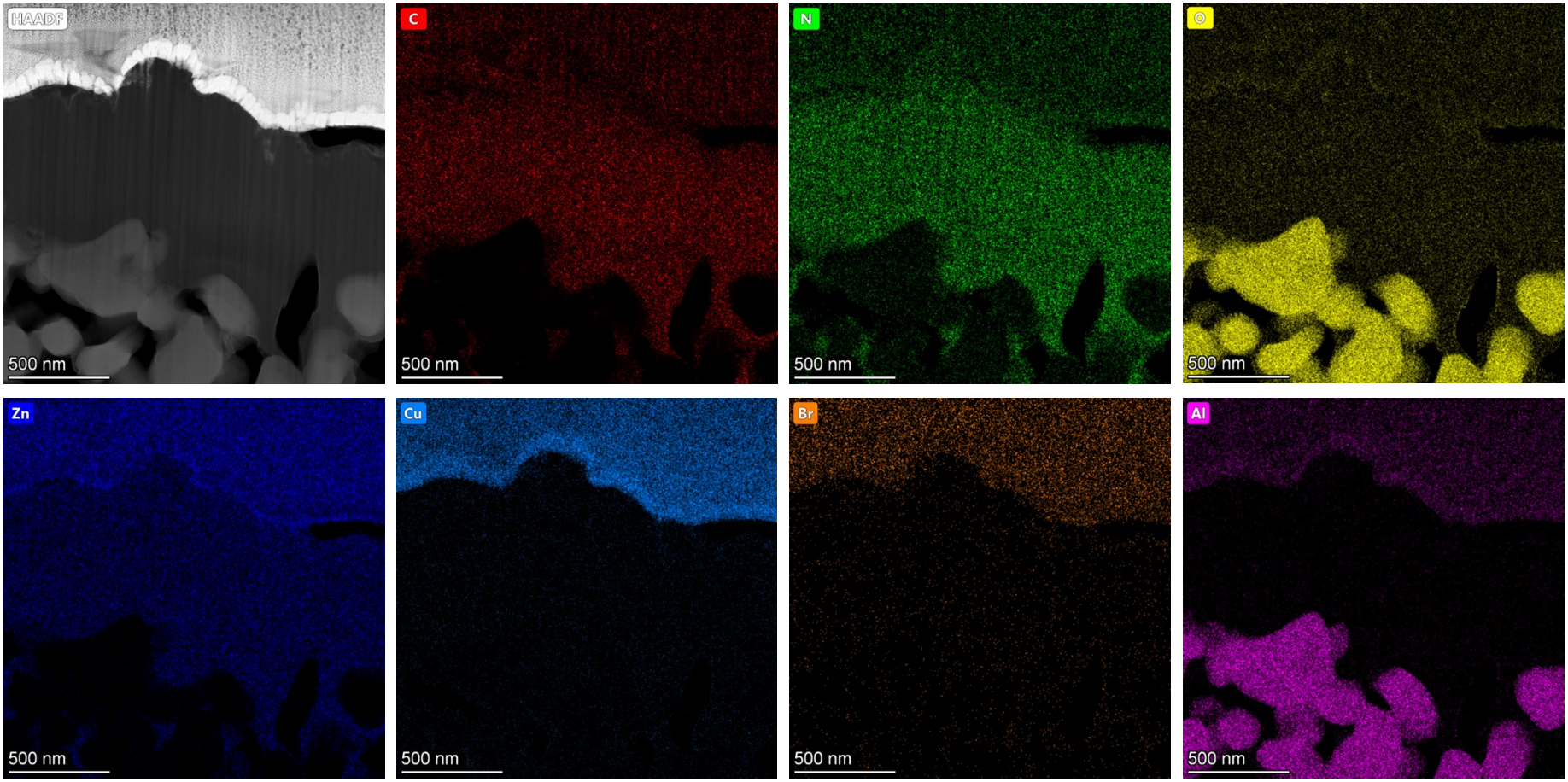

Figure S9. EDX elemental mapping images of a ZIF-8-PMMA membrane.

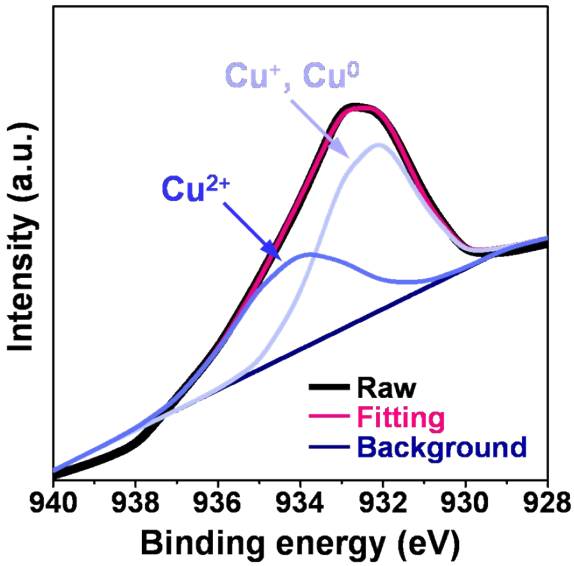

Figure S10. Cu 2p3/2 XPS spectra and deconvoluted curves of a ZIF-8-PMMA membrane.

Table S1. Permeation data measured at room temperature and ~ 1 atm.

Sample	No.	C_3H_6 permeance (mol m^{-2} s^{-1} Pa^{-1})	C_3H_8 permeance (mol m^{-2} s^{-1} Pa^{-1})	C_3H_6/C_3H_8 separation factor
ZIF-8	1	4.04×10^{-8}	4.57×10^{-10}	88.5
	2	3.76×10^{-8}	6.31×10^{-10}	59.6
	3	4.47×10^{-8}	10.6×10^{-10}	42.1
	Ave.	$4.31 \pm 0.53 \times 10^{-8}$	$7.17 \pm 2.54 \times 10^{-10}$	60.1 ± 13.9
ZIF-8-BiB	1	3.35×10^{-8}	5.80×10^{-10}	57.8
	2	3.33×10^{-8}	7.53×10^{-10}	44.3
	3	3.07×10^{-8}	8.66×10^{-10}	42.1
	Ave.	$3.25 \pm 1.57 \times 10^{-8}$	$7.33 \pm 1.44 \times 10^{-10}$	44.4 ± 6.6
ZIF-8-PMMA	1	4.23×10^{-8}	3.97×10^{-10}	106.6
	2	7.82×10^{-8}	7.42×10^{-10}	105.3
	3	4.68×10^{-8}	4.47×10^{-10}	104.7
	Ave.	$5.58 \pm 1.82 \times 10^{-8}$	$5.29 \pm 1.86 \times 10^{-10}$	105.5 ± 2.8

Table S2. Permeation results of ZIF-8 membranes and the corresponding ZIF-8-PMMA membranes.

Sample	MMA (mmol)	ZIF-8		ZIF-8-PMMA	
		C_3H_6 permeance (mol m^{-2} s^{-1} Pa^{-1})	C_3H_6/C_3H_8 separation factor	C_3H_6 permeance (mol m^{-2} s^{-1} Pa^{-1})	C_3H_6/C_3H_8 separation factor
S1	0.14	6.39×10^{-8}	4.2	5.35×10^{-8}	6.1
S2	0.14	3.79×10^{-8}	21.0	4.33×10^{-8}	54.3
S3	0.14	4.38×10^{-8}	61.3	5.57×10^{-8}	105.6
S4	0.28	4.74×10^{-8}	58.1	2.94×10^{-8}	108.8
S5	0.69	5.62×10^{-8}	3.2	1.79×10^{-8}	59.6
S6	0.69	4.17×10^{-8}	9.8	1.47×10^{-8}	90.9
S7	0.69	4.46×10^{-8}	66.0	1.20×10^{-8}	100.5

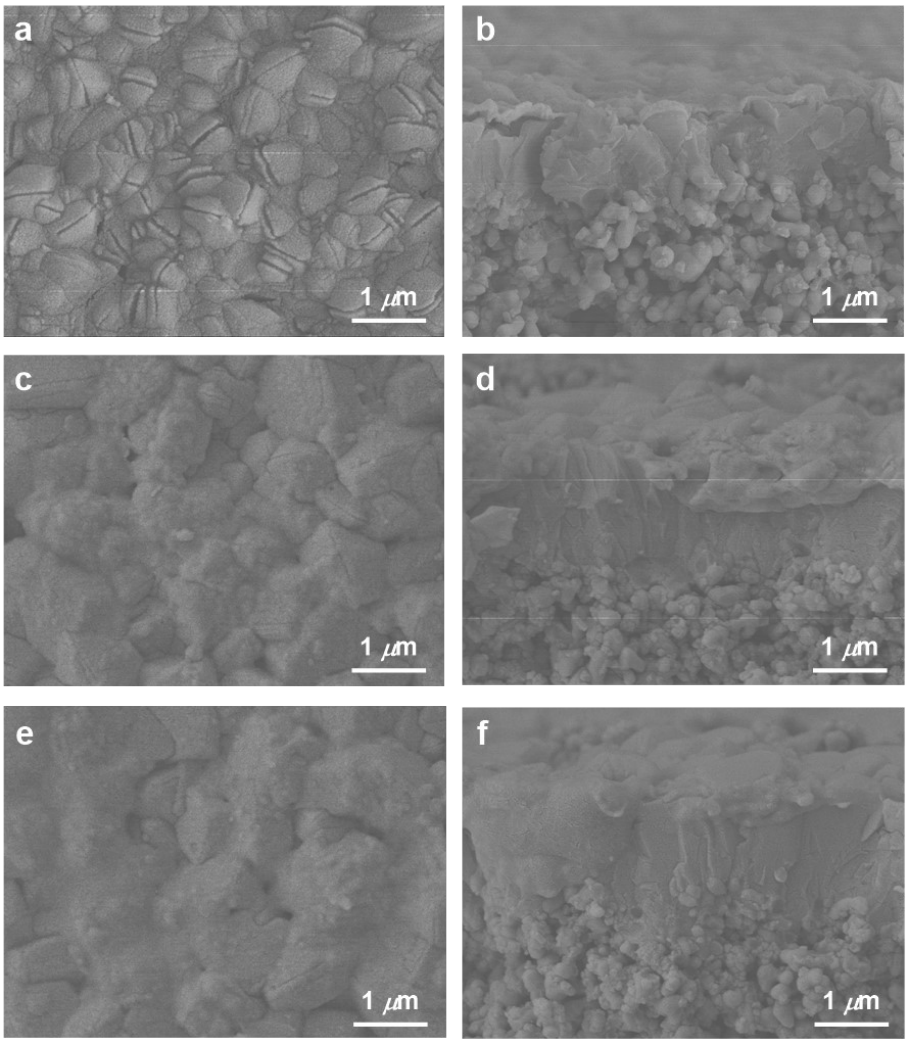

Figure S11. SEM images of ZIF-8-PMMA membranes with different PMMA thicknesses controlled by the contents of MMA during the ATRP step. The MMA content varies from 0.1 mmol (**a**, **b**), to 0.3 mmol (**c**, **d**), and to 0.7 mmol (**e**, **f**). On the left are the top views and on the right the cross-sectional views.

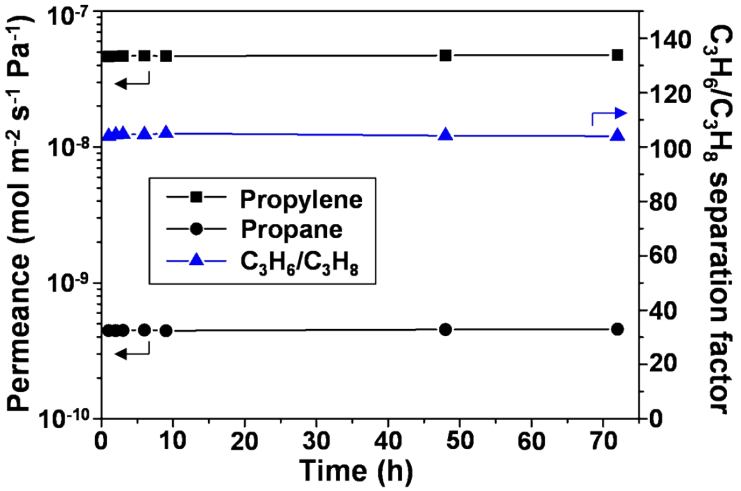

Figure S12. Long-term C_3H_6/C_3H_8 separation performance of the ZIF-8-PMMA membrane.